ELMs Observed at the Targets of an Axisymmetric Divertor

Michael Laux[1], Stefan Jachmich[2], Albrecht Herrmann[1],
Thomas Eich[3] and
contributors to the EFDA-JET workprogramme

[1]Max-Planck-Institut für Plasmaphysik, Association EURATOM,Germany
[2]Laboratory for Plasma Physics,Ecole Royale Militaire/Koninklijke Militaire School,
Association EURATOM-Belgian State, Brussels, Belgium
[3]Institut für Plasmaphysik FZ Jülich, Association EURATOM, Trilateral Euregio Cluster, Jülich, Germany

Abstract

The non-linear disturbances of the divertor plasma caused by ELMs are observed by a number of divertor diagnostics. A dedicated averaging procedure is applied to the time traces of the signals to reveal the coherent behaviour in the ELM as well as the changes of ELM parameters during the ELM series. In typical ELMs saturation current I_{sat} and D_α emission behave accordingly, but temporal evolutions are different in the outer and inner divertor legs. T_e and V_{float} vary strongly during the early ELM phase where I_{sat} rises. The power flux to the target and the plasma potential can be constructed from the averaged signals. They show a remarkably smooth behaviour so that even the radial electric field along the plate can be estimated. Double peaks appearing sometimes in the power flux are seen by the thermography as well. Radial profiles of I_{sat} and I(U)-characteristics of single probe tips could be reconstructed using the ELM times for a sorting procedure.

Introduction

To monitor the spatial distribution and temporal evolution of the saturation current I_{sat}, electron temperature T_e, and the floating potential V_{float}, arrays of Langmuir probes have been built into the target plates of the axisymmetric divertors of JET and ASDEX Upgrade [1,2]. Furthermore, fluxes of particles and power and the plasma potential could be inferred from the directly measured parameters using simple model assumptions. As the probes are arranged in an array, profiles and spatial gradients of parameters have also been estimated.

At higher heating powers divertor tokamaks operate in the high-confinement mode (H-mode). Modes localized in the edge region (ELMs), periodically appear in H-mode plasmas in the form of short transient pulses of particles and energy passing the separatrix into the scrape-off layer (SOL), afterwards being transported into the divertor [3,4]. The particle fluxes and heat energy loads which accompany ELMs can cause losses in density and plasma energy, as well as damages of the divertor target plates. In the past the global properties and scalings of the ELMs have been explored [5,6]. However, the underlying physics is still concealed due to the stochastic nature, of which ELMs are. In order to reveal detailed information about the evolution of a typical ELM, a new ELM identification algorithm has been applied to ELMy H-mode periods in order to find ELM footprints in the D_α signal, and I_{sat}, V_{float}, and T_e from triple probes in the divertor.

Once the ELM-events of a series have been identified, the local ELM frequency, the width, height and integral of the ELM burst, and the average signal between ELMs are

calculated for every individual ELM. In addition, the data of all ELMs belonging to the same phase of the local ELM, are combined and averaged. To discover and exclude irregular ELMs their total deviation from the averaged ELM is determined.

For the calculation of more complex plasma quantities consisting of signals from different diagnostics, one signal is used as a marker and a second one is averaged along the first one. In most cases the D_α recycling has been used as a marker signal, since it usually shows a very sharp peak.

Electrical probes react especially sensitive to ELM events because ELMs are accompanied by electric fields and currents in SOL and divertor [5,6]. But it can be expected that a diagnostic suffering from a specific disturbance is generally able to provide information on the physical nature of this disturbance too.

Extraction of Coherently Averaged ELM Signals

ELM series show repititive as well as stochastic aspects. To separate both a special technique was developed that as a first step evaluates a coherently averaged ELM and reveals then the evolution of certain ELM characteristics for thethe chain of individuals in a given ELM-series. The averaging procedure needs a measured parameter (the so-called marker) that can be used as ELM indicator in the sense that an easily recognizable feature of it (like e.g. the peaking) is believed to be rigidly related to a distinct moment of time during any individual ELM (fig. 1a).
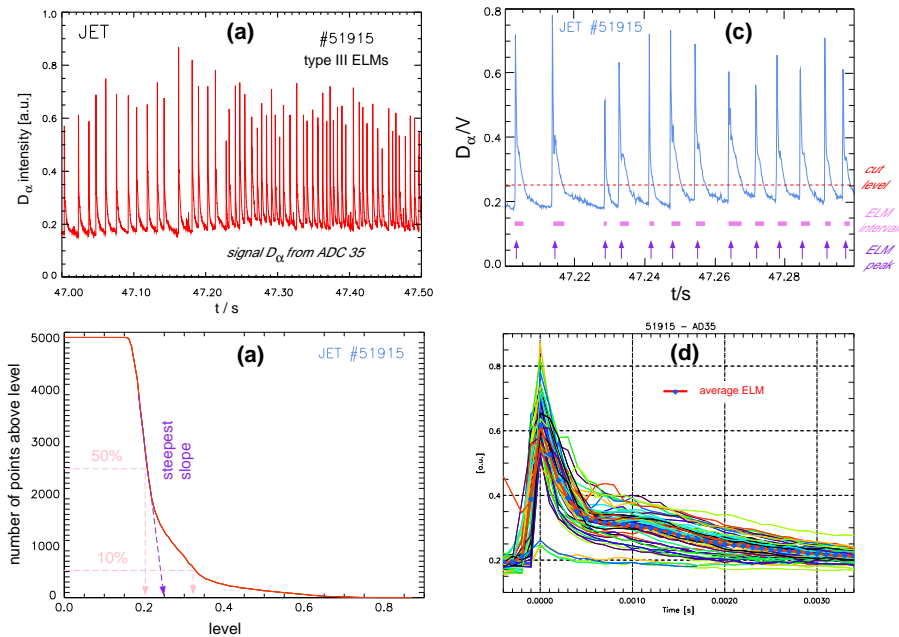

Figure 1: (a) example of a D_α ELM series, (b) distribution of values (selected cut levels indicated),(c) cut level in the ELM series (ELM intervals and maxima indicated), (d) coherently overlayed individual ELMs

The overall number of marker-signal datapoints above a given signal-level as a function of that level was constructed in Fig. 1b. A location on the slope is selected as cut level for the whole time series (in analogy to the method of pulse height analysis in nuclear physics). Even though the choice is slightly arbitrary (depending on the kind of ELMs to be accepted) it can be checked using the standard deviations for the ELM series
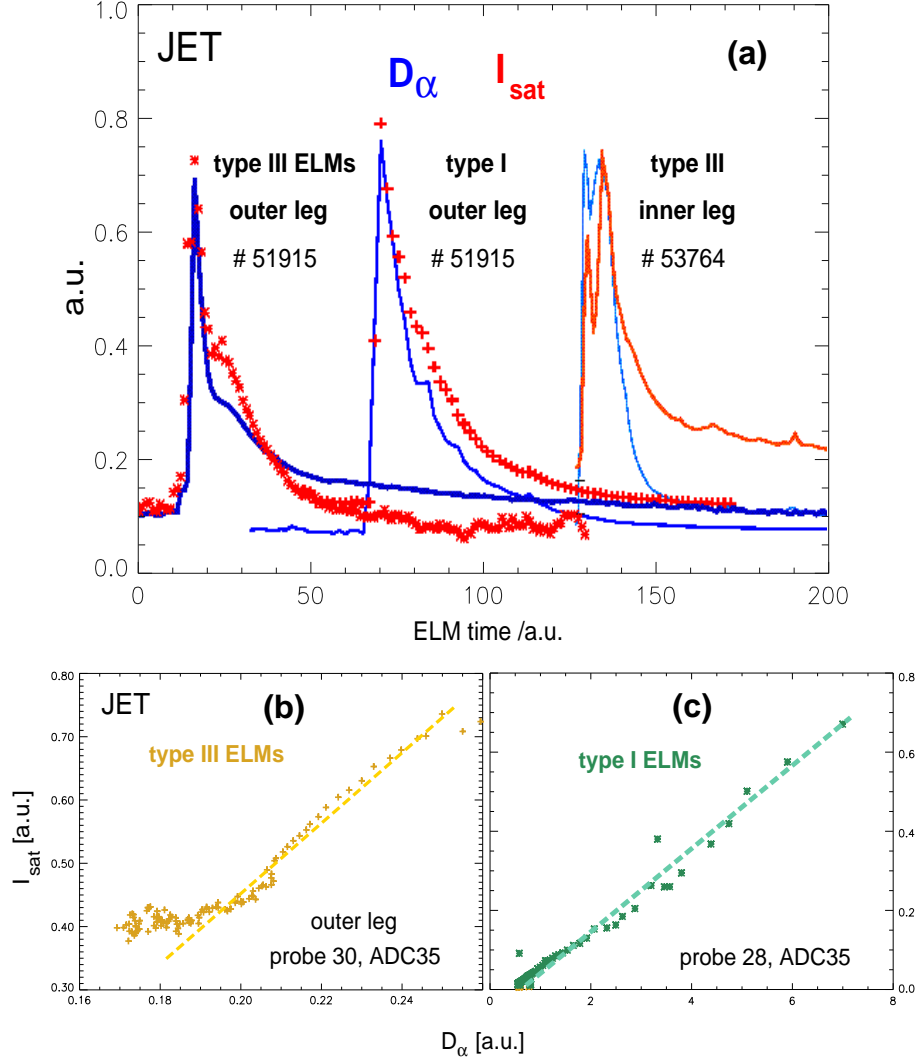
Figure 2: (a) coherently averaged D_α and I_{sat} ELMs,(b,c) coherently averaged I_{sat} vs. D_α ELM

described below. In general the method needs no prior knowledge as e.g. a preliminary estimate of the ELM frequency. In the following this cut level can be used to determine ELM intervals in the time-series of any parameter measured during the same ELMy phase (fig. 1c). These intervals then contain just one ELM and a time tick marking the selected moment of time in that ELM (like e.g. the maximum) can be determined. Afterwards all intervals of the considered signal can be overlayed with respect to the marker tick and averaged to produce a coherently averaged ELM-trace of that signal (fig. 1d).

In essence coherent averaging on the one hand reduces the noise by smearing out ELM to ELM changes and extracts the typical behaviour for the whole ELM series. On the other hand principal moments (the integral over the signal, the maximum value and its location) can be calculated for every individual ELM in the series. Using the average ELM the standard deviation of individual ELMs can be estimated with respect to the average as a figure of merit to identify outliers or recognize different kinds of ELMs in the series. Of course the ELM identification part of the methode can also be applied to unravel the disturbing interference of ELMs in all kinds of slow variations

(like slow motions of the strike zone position or slow ramps of the probe voltage). As an example fig.1 shows the D_α intensity for the outer divertor leg of JET (a) together with the functional dependence of the number of points exceeding a given level for that time series (b). The different signal levels within an ELM and in between ELMs allow the determination of a cut level that defines the intervals of all individual ELMs. The maximum D_α-signal in every interval then selects the marker ticks (c). Based on the field of these marker ticks every time series observed during the same ELMy periode can be coherently averaged now (d).

Examples of Coherently Averaged ELM Signals

Averaged ELMs of types III and I from the D_α marker signal itself and from an I_{sat} slave are shown in fig. 2a for the inner and outer divertor legs of JET demonstrating the remarkable noise reduction. The comparison of the D_α and I_{sat} ELMs show good correspondence of the two signals representing more or less directly the particle flux. Even double structures or pedestals during later ELM-times appear in both reconstructions (figures 2b,c demonstrate a linear dependence directly).
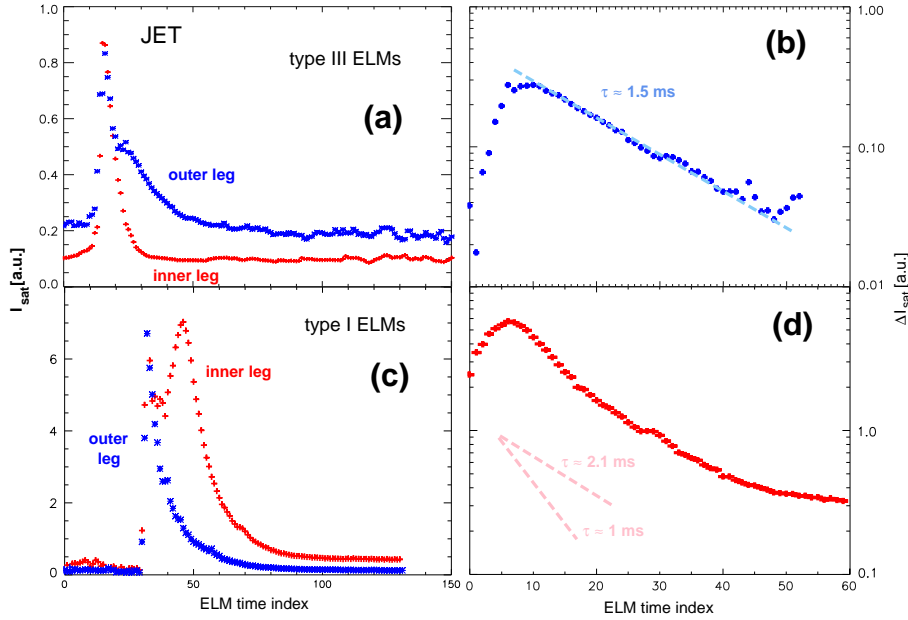

Figure 3: (a,c) I_{sat} ELMs for inner and outer leg, (b,d) exponentially decaying second components

A comparison of the averaged I_{sat} signals observed by probes situated in the SOL just outside separatrix in the inner and outer legs of JET allows to postulate a second component to the outer leg in a type III ELM-series (fig.3a). This component behaves clearly exponential in time ($\tau \approx 1.5ms, fig.3b$). For type I ELMs a large additional component to the inner leg was observed (fig. 3c) that behaves close to exponential ($\tau \approx 1...2.1ms, fig.3d$). If the differences observed are due to a generally different behaviour of the distinct ELM types or brought about by different power fluxes crossing the separatrix or different density and mean free path has to be investigated further.

In the divertor of ASDEX Upgrade the influence of ELMs has partly a different character. During the early phase of an AUGD type I ELM a short highly turbulent period exists that is found in D_α and I_{sat} even after averaging over more than 1000
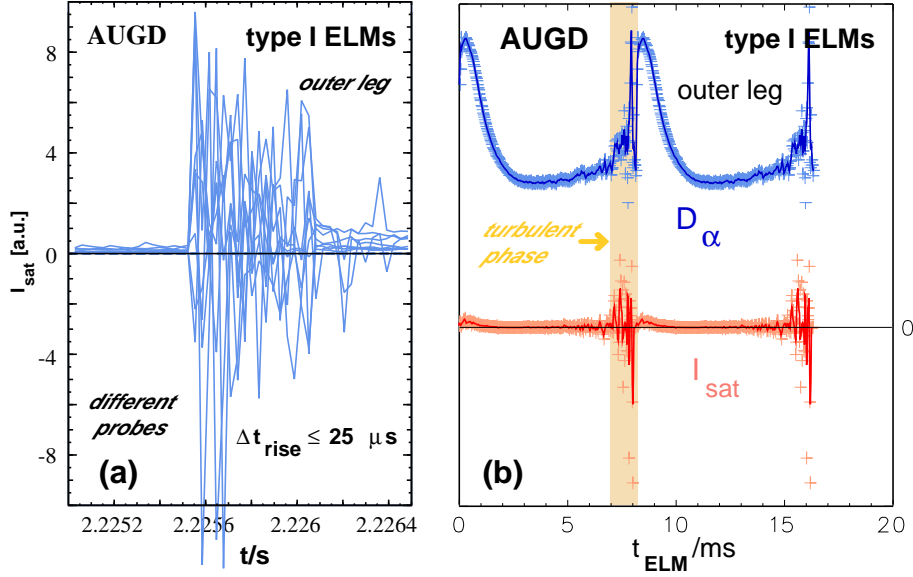
individual ELMs (fig.4a).

Figure 4: (a) I_{sat} from different probes early in the ELM, (b) coherently averaged D_α and I_{sat} ELMs in AUGD

Outside that periode the averaged ELM signals are very smooth and free of noise. Most remarkable is the fact that the ion saturation current does change sign during the turbulent periode, thereby loosing its original physical meaning. Although this behaviour is very pronounced for all probe signals at ASDEX Upgrade we could detect the very noisy ELM phase also in the averaged D_α ELM in the outer divertor (fig. 4b). At JET no such turbulent behaviour is observed, but averaging T_e or V_{float} reveals that both signals also peak clearly during the rise phase of the accompanying I_{sat} showing large excursions (cf.9a).
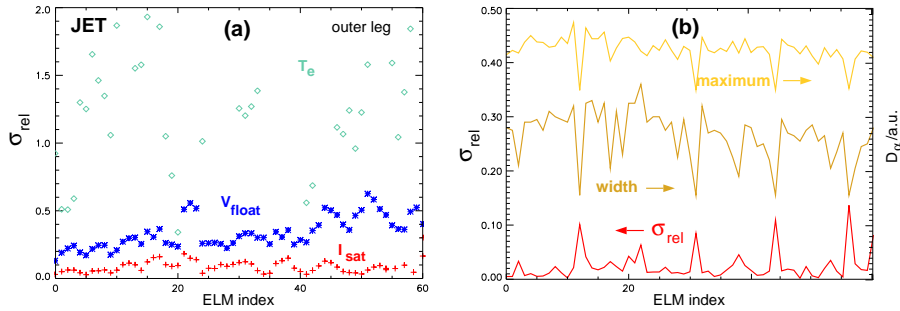

Figure 5: (a) rel. deviation for T_e, V_{float} and I_{sat}, (b) rel. dev. , maximum and peak width for a D_α ELM series

The individual standard deviation of the D_α ELMs with respect to the averaged one is very small (2-6%!, see Fig. 5b). This proves that the averaged ELM is in fact the typical ELM of this series. However it becomes also clear that there are four exceptional ELMs present. Regular ELMs seem to be interspersed with those short and small additional peaks having a surprisingly regular time pattern with a period of 77 ms, which is much lower than the actual ELM-frequency.

Fig. 5a shows that the deviation of the I_{sat} ELM from the average is also reasonably small (5-10%), but for V_{float} and T_e it is much higher (10-40% and 30-200%, respectively).

Changes of Individual ELM Parameters During H-mode Discharges

From a standard H-mode discharge (I_p= 3 MA, P_{tot} = 15 MW, n=2.8 10^{19} m^{-3}) the series of ELMs has been extracted and analysed (fig.6a). It is obvious that the ELM-frequency is slightly increasing with time (fig. 6b). A simple relation between the time span since the last ELM and the peak area of the subsequent ELM seems to hold at least in a statistical sense (fig. 7a).
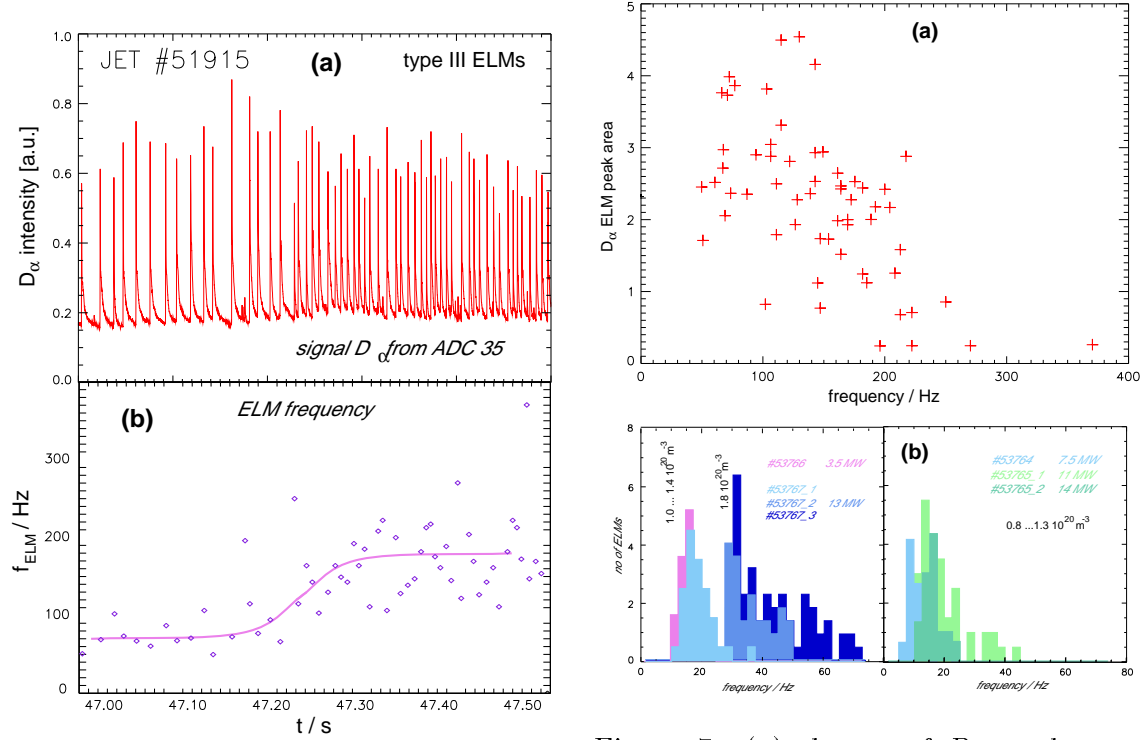

Figure 6: (a) D_α ELM series in JET shot 51915, (b) changing ELM frequency

Figure 7: (a) change of D_α peak area with ELM frequency, (b) distrib. of ELM frequ. for different density and NI power

The postulate that more particles accumulate until the next ELM-event is triggered, leads to an inverse proportionality between the peak area and the ELM-frequency confirming the decrease of the D_α peak area with the inverse time between ELMs.

Comparing ELM frequencies for discharges having different line averaged density and neutral beam power it seems that the former has a much clearer influence (fig.7b). Even if the NI power changes at JET from 3.5 to 13 MW the effects on the ELM frequency are within the width of the distribution.

If strong gas-puffing is applied the ELM peaks are broadened (Fig. 8a). Although the neutral gas has been released into the base of the inner divertor the outer divertor recycling appears to be influenced as well.

At low power crossing the separatrix or at low densities a double peak (seen sometimes in the heat power flux by thermography) can also be present in I_{sat} as illustrated in Fig. 8b. Comparison with the D_α has confirmed this observation.
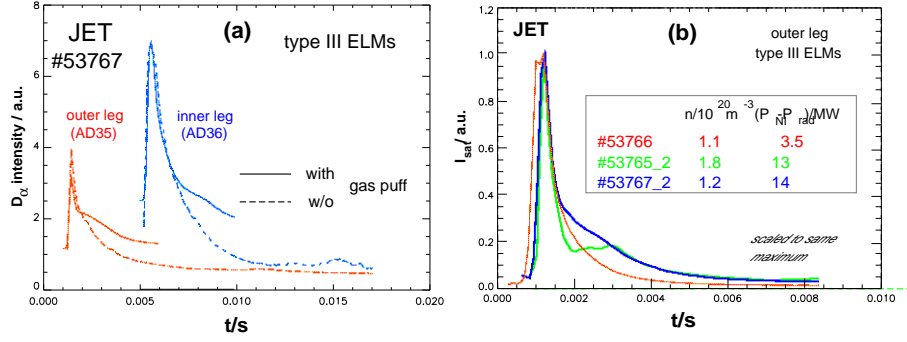
Figure 8: (a) coherently averaged D_α ELMs with and w/o gas puff, (b) I_{sat} ELMs for different densities and NI power

In some cases the post-ELM signals do not return to their pre-ELM values until the next ELM approaches and, therefore, higher particle fluxes and temperatures can built up. This non-stationary behaviour usually leads to a type transition.

Using two or more adjacent probe tips at different distances to the strike point the local gradient length of I_{sat} can be estimated (fig. 11b). The gradient of the SOL profile of I_{sat} is higher in the ELM burst than in between ELMs.
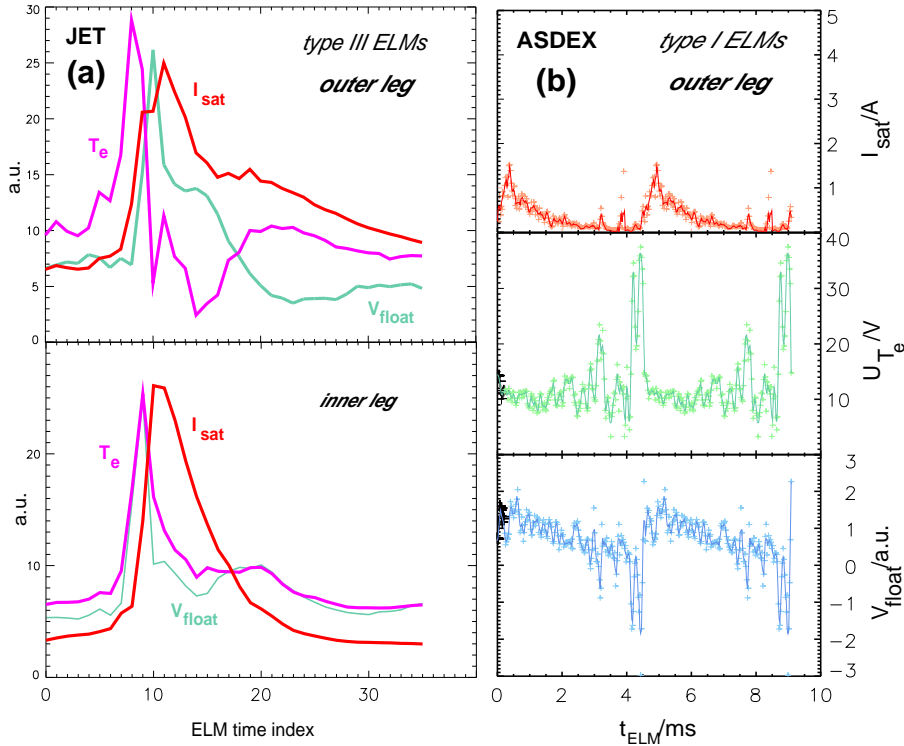

Figure 9: averaged ELMs of T_e, V_{float} and I_{sat} in JET (a) and AUGD (b)

Detailed temporal evolution of an ELM

T_e and V_{float} peak during the rise of I_{sat} (Fig. 9). Because of the structure of the T_e evolution and the shift of its peaking with respect to the I_{sat} maximum the temporal

evolution of the deduced power to the plate (using a conservative sheath transmission factor γ of 8, assuming $T_i = T_e$) can be very complex. The early rise of T_e leads to a broadening or even to a multi-peak structure of the power load (Fig. 10a).
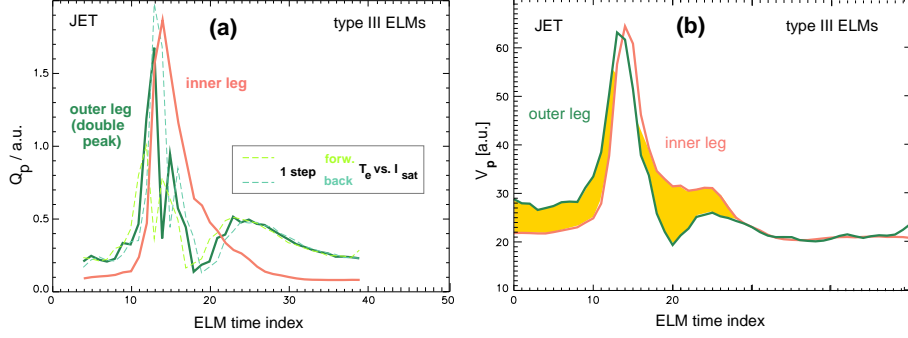

Figure 10: (a) reconstructed ELM of the power flux density from probes, (b) reconstructed ELM of the plasma potential from probes

Although the electrons reach up to 30-40 eV, the applied voltage is sufficient to measure the I_{sat}. So the calculated power flux represents the heat flow due to the electrons. Despite a possible change of γ caused by a higher T_i/T_e, the rate of change is small enough to assure a good measurement of Q_p. Since no probe was located at the seperatrix, it is not possible to derive the spatially maximum power load. Nevertheless it can at least be concluded that the power load onto the inner target is significantly higher than to the outer, because the inner probe is farther away from the separatrix than the probe at the outer one. Between the ELMs the ratio might be vice-versa. Measurements of the power flux from divertor IR-data support this important result [9].

Presuming a simple model for the sheath the plasma potential during the type III ELM in JET was calculated and found to be unexpectedly simple (fig.10b). As a next step plasma potentials have been constructed for neighbouring target probes in the outer leg of the JET divertor giving the typical evolution of the radial electric field (fig. 11a).
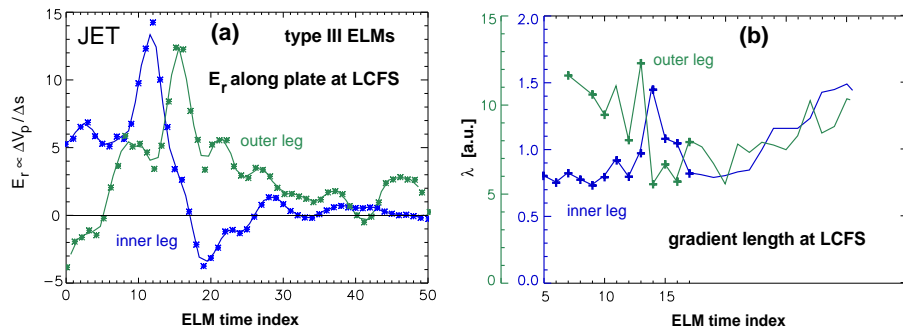

Figure 11: (a) reconstructed radial electric field, (b) reconstructed gradient length of I_{sat} from probes

Radial Profiles and Probe Characteristics by ELM Sorting

A shift of the plasma column is applied to change the relativ position of the measuring probes with respect to the position of the strike point at the divertor plate. This leads to a more complete profile. The time series of probe signals (fig. 12 b-d) and the strike

point position (fig. 12 e) for an ELMy H-mode in ASDEX-Upgrade have been sorted regarding to the time span since the last ELM, given by the evaluation of the marker signal (fig. 12 a).
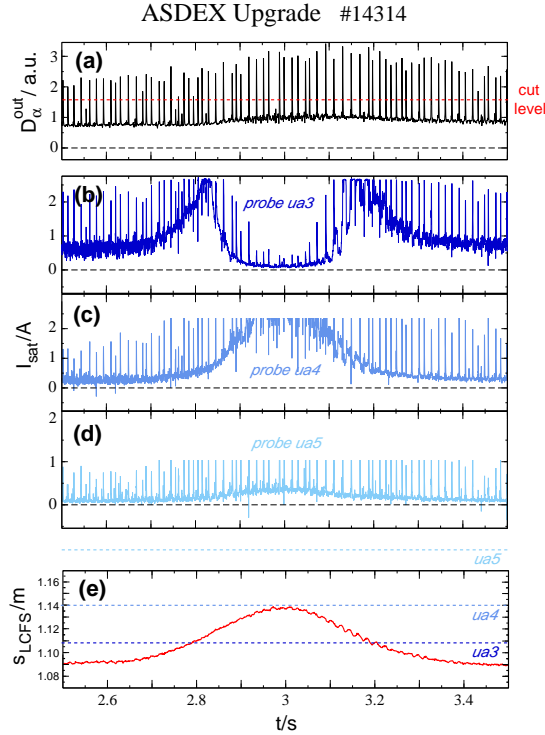

Figure 12: I_{sat} and D_α ELM series in ASDEX-Upgrade shot 14314 and the shifting position of the strike point
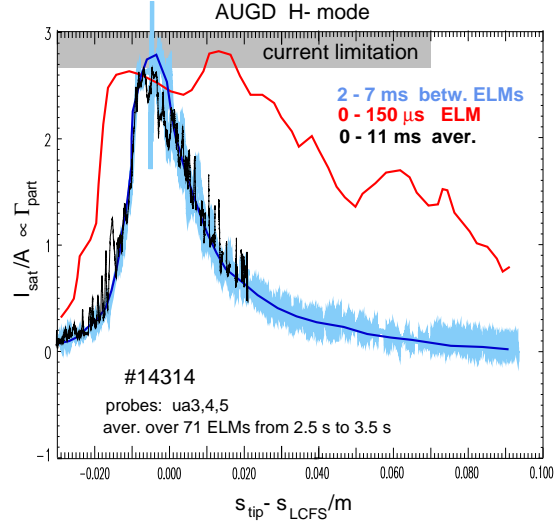

Figure 13: sorted I_{sat}-profiles between ELMs, at ELM maximum and averaged over the ELM

The result can be used to construct lateral profiles for different pre-selected time windows during the averaged ELM. Fig. 13 shows I_{sat} profiles at the ELM maximum, between ELMs, and averaged over the whole ELM duration except the early turbulent phase mentioned above. It has to be taken into consideration that a limitation for the current measurement exists at 2.5 to 3 A depending on the measuring resistance. The profile pieces from the three tips contributing, match very well giving a reliable and complete profile along the outer divertor plate. At its maximum the typical ELM exhibits a much broader profile compared with the phase between ELMs, but the short duration of the ELM peaking leads only to minor corrections if the profile is averaged over the ELM.

If probe tips are used in single probe mode by applying a voltage ramp, the probe current (fig. 14b) and the voltage (fig. 14c) can be sorted according to the ELM markers signal (fig. 14a) to extract voltage-current characteristics for the different phases during the typical ELM event.

Fig. 15 shows the probe characteristics between ELMs and at the ELM peak as examples. It seems that understandable IU-characteristics can be observed for voltages between $\approx -30V$ and $\approx +25V$ in both cases. For voltages below $-30V$ the currents are very large and noisy and the overall behaviour reminds that during arcing events at a probe sometimes observed in the past. Above $+25V$ the current is systematically reduced and the noise level is also high. There are theories of the probe behaviour in strong
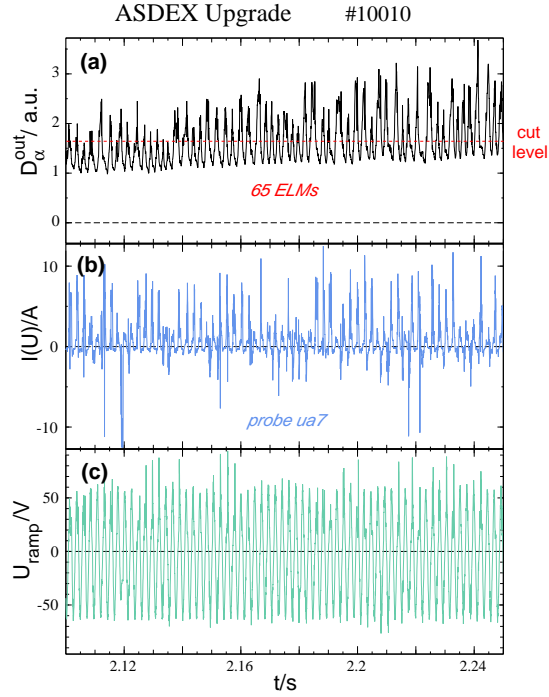
Figure 14: ramp voltage U, probe current I, and D_α during an ELM series in ASDEX-Upgrade shot 10010
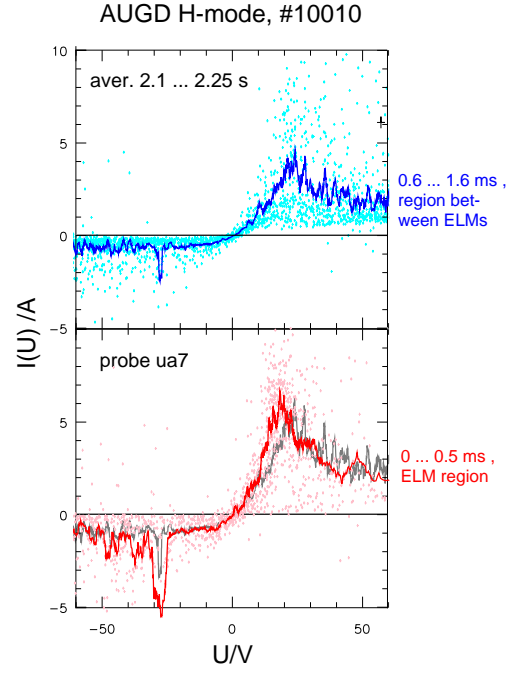
Figure 15: sorted IU-characteristics between ELMs and at ELM maximum

magnetic fields ([10]) which forecast a breakdown of the otherwise existing stationary solution for the problem at positive probe voltages exceeding a certain critical one.

Conclusions

The coherent averaging methode is able to study ELMs in a more systematic manner and deliver the temporal evolution of plasma parameters during an ELM. The averaged I_{sat} and D_α are usually linearly related throughout the ELM. As a consequence of the noise reduction distinct components to I_{sat} and D_α could be identified. Additionally, reliable temporal evolution of the plasma potential, the power flux to the target, the gradient length close to the strike point, and the radial electric field has been derived for JET. A turbulent phase was identified during the ELM rise (more pronounced at AUGD than at JET) seriously challenging the probe interpretation.

The relatively small standard deviations of the single ELMs from the averaged one demonstrate clearly the existence of a typical ELM and have proven that such an analysis is reasonable. The technique can be applied to any measured quantity and thus allows the calculation of even more complex plasma quantities. A first analysis has shown an early rise in T_e and V_{float}, which is in contrary to the delayed I_{sat}-rise and, therefore, causes a double peak structure in the power load. The heat flux consists of two components: an early short small pulse of hot particles, followed by a longer large one at much lower temperature. The study of inner/outer divertor recycling asymmetries has elucidated particle fluxes, which appear after the ELM burst at longer time scales. Depending on the density and gas puffing, they are seen either on the outer or the inner divertor box.

In order to retrieve more information the procedure is extended to slow X-point sweep and slow probe voltage ramps. In the first case changes of the SOL-profiles during an ELM can be reconstructed for each ELM time, in the second I(U)-characteristics can be analysed. It was found that the radial profiles are broader for the ELM core than for later phases in good agreement with coherently averaged gradient lengths derived with a few probes close to the separatrix.

Classical probe characteristics do exist during the whole ELM (except the a possible turbulent phase) if the ramp voltage is neither to small nor to large. The physics of these restrictions has to be investigated further.

References

[1] G.F. Matthews, S.D. Davies, R.D. Monk, Contrib. Plasma Phys. 36 (1996) S, 29-36

[2] M. Weinlich, A. Carlson, Contrib. Plasma Phys. 36 (1996) S, 53-60

[3] H. Zohm, Plasma Phys. Contr. Fusion 38(1996),105-128

[4] W. Suttrop, Plasma Phys. Contr. Fusion 42 (2000), A1-A14

[5] J. Lingertat, M. Laux, R.D. Monk, J. Nucl. Mater. 290-293 (2001), 896-899

[6] J. Lingertat, K. Günther, A. Loarte, J. Nucl. Mater. 220/222 (1995), 198-202

[7] JET Team, Nucl. Fusion 39 (1999), 1687

[8] G. Saibene et al., Nucl. Fusion 39 (1999), 1133

[9] Th. Eich et al., EPS 2001

[10] K. Guenther, A. Carlson, Contrib. Plasma Phys. 38 (1994)S